

## RVC OPEN ACCESS REPOSITORY – COPYRIGHT NOTICE

This is the peer reviewed version of the following article:

Gregori, T., Lam, R., Priestnall, S. L. and Lamb, C. R. (2016), TRUNCATION ARTIFACT IN MAGNETIC RESONANCE IMAGES OF THE CANINE SPINAL CORD. *Veterinary Radiology & Ultrasound*. doi: 10.1111/vru.12380

which has been published in final form at <http://dx.doi.org/10.1111/vru.12380>.

This article may be used for non-commercial purposes in accordance with [Wiley Terms and Conditions for Self-Archiving](#).

The full details of the published version of the article are as follows:

TITLE: TRUNCATION ARTIFACT IN MAGNETIC RESONANCE IMAGES OF THE CANINE SPINAL CORD

AUTHORS: Gregori, T., Lam, R., Priestnall, S. L. and Lamb, C. R.

JOURNAL TITLE: *Veterinary Radiology & Ultrasound*

PUBLISHER: Wiley

PUBLICATION DATE: 2 June 2016 (online)

DOI: 10.1111/vru.12380

1 **Truncation artifact in magnetic resonance images of the canine spinal cord**

2

3 T. Gregori, R. Lam, S.L. Priestnall, C.R. Lamb

4 Department of Clinical Sciences and Services (Gregori, Lam, Lamb) and the Department of Pathology and

5 Pathogen Biology (Priestnall), The Royal Veterinary College, Hawkshead Lane, North Mymms,

6 Hertfordshire AL9 7TA, UK.

7

8 Key words: dog, magnetic resonance imaging, spinal cord, truncation artifact

9 Running head: Truncation artifact

10

11 Funding Sources: unfunded

12 **Abstract**

13 The truncation artifact in magnetic resonance (MR) images is a line of abnormal signal intensity that  
14 occurs parallel to an interface between tissues of markedly different signal intensity. In order to  
15 demonstrate the truncation artifact in sagittal images of the canine spinal cord and the effect of  
16 changing spatial resolution, we conducted an experimental in vitro study. A section of fixed canine spinal  
17 cord was imaged using a 1.5T magnet. Spatial resolution was increased by increasing the acquisition  
18 matrix and reconstruction matrix, producing series of T2-weighted images with the following pixel sizes:  
19 A, 1.6mm (vertical) x 2.2mm (horizontal); B, 1.2mm x 1.7mm; C, 0.8mm x 1.1mm; D, 0.4mm x 0.6mm.  
20 Plots of mean pixel value across the cord showed variations in signal intensity compatible with  
21 truncation artifact, which appeared as a single, wide central hyperintense zone in low resolution images  
22 and as multiple narrower zones in high spatial resolution images. Even in images obtained using the  
23 highest spatial resolution available for the MR system, the edge of the spinal cord was not accurately  
24 defined and the central canal was not visible. The experiment was repeated using an unfixed spinal cord  
25 specimen with focal compression applied to mimic a pathologic lesion. Slight hyperintensity was  
26 observed within the spinal cord at the site of compression although the cord was normal histologically.  
27 Results of this study suggest that caution should be applied when interpreting hyperintensity affecting  
28 the spinal cord in T2-weighted sagittal images of clinical patients because of the possibility that the  
29 abnormal signal could represent a truncation artifact.

30

## 31 Introduction

32 The truncation artifact (also known as Gibbs' artifact) in magnetic resonance (MR) images is a line of  
33 abnormal signal intensity that occurs parallel to an interface between tissues of markedly different  
34 signal intensity.<sup>1,2</sup> It has been observed in MR images of various anatomic structures in humans,  
35 including the brain, spinal cord, and articular cartilage.<sup>3-5</sup> In dogs, a truncation artifact may be observed  
36 in T2-weighted (T2w) sagittal images of the spine as a single or multiple hyperintense lines  
37 superimposed on the spinal cord<sup>6-8</sup> (Figure 1). Based on the hyperintensity, shape and position of this  
38 truncation artifact, it has been suggested that it could potentially be misinterpreted as a sign of a dilated  
39 central canal or a syrinx.<sup>3,6</sup> All MR sequences are subject to truncation artifact. In T1w images, the  
40 truncation artifact appears as a hypointense band superimposed to the parenchyma of the spinal cord.  
41 Truncation artifacts cannot be eliminated completely from MR images because they occur as a  
42 consequence of the Fourier transformation used to construct the digital image from the signals obtained  
43 from a volume of tissue. Digital images contain a finite number of pixels, each with a finite dynamic  
44 range, and represent an approximation of the true signal intensity originating in tissues. Particularly at  
45 boundaries of tissues with markedly different signal intensities (e.g. tissue-fluid interfaces in T2w  
46 images), data are necessarily truncated in *k*-space, causing misrepresentation of signal intensities either  
47 side of the boundary.<sup>2,4,5,9</sup> Although it cannot be eliminated, the truncation artifact can be minimized by  
48 increasing spatial resolution (decreasing the pixel size), by applying pre-reconstruction filters (e.g.  
49 Hamming or Tukey) or by using post-processing optimization techniques (e.g. the Total Variation  
50 method).<sup>9, 10, 11</sup>

51 The present study had two aims: 1, to demonstrate the truncation artifact in MR images of the normal  
52 canine spinal cord, including the effect on its appearance of changing spatial resolution; 2, to  
53 demonstrate variations in the appearance of the truncation artifact within the spinal cord at a site of

54 compression.

55

## 56 **Material and methods**

### 57 *First part of the study*

58 To conduct the in vitro experiment, the spinal cord was removed intact from the fresh cadaver of a  
59 client –owned 7 year old, 26 kg male Boxer dog, humanely euthanized for reasons unrelated to this  
60 study. Owner consent was obtained to perform necropsy and obtain tissues from the cadaver, for  
61 research purposes.. The dura mater was removed and the spinal cord with attached pia mater and  
62 fragments of arachnoid was cut into three sections of approximately equal length and fixed in 10%  
63 neutral-buffered formalin. To simulate the spinal cord surrounded by cerebrospinal fluid (CSF), the  
64 cervical section of the spinal cord was submerged in formalin in a plastic tray and placed on a phased-  
65 array spinal coil within the bore of a 1.5T magnet (Intera Pulsar System, Philips Medical Systems,  
66 Reigate, UK). Turbo spin-echo (TSE) sequences were used to obtain sagittal T2w (T2w) images with the  
67 following settings: echo time 120ms, repetition time 3154ms, 10 signals averaged, and field of view  
68 102mm (vertical) x 159mm (horizontal long axis) x 26mm (right to left). A default ringing pre-  
69 reconstruction filter was used to reduce truncation artifact on the images obtained. Spatial resolution  
70 was progressively increased by increasing the acquisition matrix and reconstruction matrix, producing  
71 series of T2w images with the following pixel sizes: A, 1.6mm (vertical) x 2.2mm (horizontal); B, 1.2mm x  
72 1.7mm; C, 0.8mm x 1.1mm; D, 0.4mm x 0.6mm. Slice thickness was 1.8mm for each series. Series B  
73 used the default spatial resolution settings used at our institution for acquiring T2w TSE sagittal images  
74 of the spine of clinical canine patients of similar size to the cadaver used. Series D represented the  
75 highest spatial resolution available on this MR system. Transverse images of the spinal cord were also  
76 acquired using the same spatial resolution as series A.

77 For each series (A-D), sagittal MR images of the spinal cord were viewed at native resolution (i.e. not  
78 interpolated) and a 6-pixel wide region of interest (ROI) was selected from the central portion of the  
79 spinal cord that was parallel to the horizontal axis of the image. The ROI was placed over the same part  
80 of the cord in each image. This ROI was re-windowed so that the minimum pixel value was 0 and the  
81 maximum was 255, and the mean pixel value was calculated for each line of pixels across the spinal  
82 cord. A graph of pixel value was produced for each scan and aligned with the corresponding image of  
83 the spinal cord (Figure 2).

84 Following MR imaging, representative hematoxylin and eosin-stained histologic sections of the spinal  
85 cord were prepared and reviewed. The height and width and of the spinal cord and the sagittal diameter  
86 of the central canal were measured using an eyepiece graticule.

#### 87 *Second part of the study*

88 An unfixed section of the cervical spinal cord from the fresh cadaver of a client-owned 5 year old, 30 kg  
89 male Greyhound dog was submerged in physiologic saline in a plastic tray. Owner consent was obtained  
90 to perform necropsy and obtain tissues from the cadaver, for research purposes. Two empty 5 ml plastic  
91 syringe barrels placed on either side of the spinal cord and held together using elastic bands were used  
92 to create focal compression of the spinal cord. Sagittal T2w images were obtained with the following  
93 settings: echo time 120ms, repetition time 3085ms, 10 signals averaged, and field of view 69mm  
94 (vertical) x 106mm (horizontal long axis) x 22mm (right to left). Four images series with the following  
95 pixel sizes were obtained: series A2, 1.6mm (vertical) x 2.3mm (horizontal); series B2, 1.1mm x 1.5mm;  
96 series C2, 0.8mm x 1.1mm; series D2, 0.4mm x 0.5mm. Slice thickness was 1.8mm for each series.

97

## 98 **Results**

#### 99 *First part of the study*

100 A broad zone of increased signal, compatible with a truncation artifact, was evident along the midline of  
101 the spinal cord in all T2w TSE sagittal images. The zones of abnormal signal intensity associated with  
102 truncation artifact within the spinal cord and in the surrounding saline were relatively wider (up to  
103 2mm) in images acquired at lower resolution (Figure 3). With increasing spatial resolution the zones of  
104 abnormal signal intensity became narrower and less intense, so that the apparent outer border of the  
105 spinal cord became more clearly defined. The abnormal signal within the spinal cord appeared as a  
106 single, wide central zone in low resolution scan images and as multiple narrower zones in images with  
107 higher spatial resolution. In transverse images of the spinal cord acquired using the same spatial  
108 resolution as scan A, multiple concentric zones of abnormal signal intensity were evident. Compared to  
109 a gross section of the cord, the apparent diameter of the spinal cord in transverse images was greater  
110 and the central canal was not visible (Figure 4). No spinal cord lesions were identified pathologically.

#### 111 *Second part of the study*

112 In the areas where the spinal cord was not compressed the truncation artifact had a similar appearance  
113 in both sagittal and transverse images to that described in the first part of the study. In the lower  
114 resolution images (series A2, B2, C2) concentric truncation artifacts emanating from the two syringe  
115 barrels overlapped the spinal cord, impeding evaluation of the signal intensity of the spinal cord at the  
116 site of compression (Figure 5A-C). In the highest resolution images (series D2), the spinal cord at the site  
117 of compression had slightly increased signal intensity, apparently as a result of merging of hyperintense  
118 lines associated with truncation artifact (Figure 5D). This appearance may be compared with the  
119 increased signal that observed at sites of spinal cord compression in clinical patients (Figure 6).

120

#### 121 **Discussion**

122 In low resolution MR images, the central hyperintense zone caused by the truncation artifact is much

123 wider than the central canal. Within increasing spatial resolution, the hyperintensity associated with the  
124 truncation artifact appeared as multiple parallel zones in both sagittal and transverse images. This  
125 variation is compatible with previous experimental results that showed the truncation artifact to be a  
126 function of resolution relative to the dimensions of the object being imaged.<sup>3</sup> Constructive interference  
127 between the signal intensity waveforms produced on each side of an object can produce different  
128 numbers of peaks and troughs depending on the separation of the two borders of the object and the  
129 pixel size of the image.<sup>3</sup> Similarly, reduced cord diameter at sites of compression alters the appearance  
130 of the truncation artifact from multiple hyperintense zones into a single broad zone, as observed in the  
131 second part of study. In sagittal T2w images of the cervical spine of clinical patients, variation of the  
132 truncation artifact may also account for the hyperintensity observed in the spinal cord where it narrows  
133 at a site of compression; the abnormal signal intensity identified on this sequence should therefore be  
134 interpreted with caution.

135 The truncation artifact should be easy to recognize when it appears as multiple lines, but when it  
136 appears as a single hyperintensity it may be more difficult to distinguish from a lesion. This pitfall has  
137 been noted in MR images of articular cartilage<sup>4</sup>, the menisci of the knee<sup>12</sup> and the spinal cord, in which a  
138 linear truncation artifact could be confused with hydromyelia or syringohydromyelia.<sup>3</sup> In a study of dogs  
139 with cervical disc disease, occurrence of the truncation artifact was thought to contribute to  
140 interobserver variations.<sup>7</sup> Although truncation artifacts are encountered in other MR sequences, it is the  
141 fact that they appear hyperintense when superimposed on neural tissues in T2w images that is  
142 problematic because most neural lesions are also hyperintense in T2w images. When uncertainty exists  
143 about whether a hyperintensity affecting the spinal cord may represent a lesion, additional imaging is  
144 indicated. For example, increasing spatial resolution (by increasing matrix size and/or decreasing field of  
145 view) will reduce the magnitude of the artifact.<sup>6</sup> If the image matrix is asymmetrical, aligning the critical  
146 boundary perpendicular to the higher frequency axis (usually the frequency-encoding direction) will



147 diminish the truncation artifact.<sup>2</sup> Obtaining images in a different plane, such as transverse images,  
148 should also be considered if this reduces imaging across a boundary between tissues of markedly  
149 different signal intensity; however, for the spinal cord, sagittal, dorsal, and transverse images will be  
150 affected by truncation artifacts to a similar degree because the critical spinal cord-CSF boundary cannot  
151 be avoided.

152 In the present study, images were acquired of fixed spinal cord so that measurements based on MR  
153 images could be directly compared to measurements from histologic specimens without errors  
154 introduced by shrinkage of tissues during fixation. One disadvantage of this approach is that the signal  
155 intensity of the fixed spinal cord in T2w images is reduced compared to the cord in vivo because of  
156 removal of water during fixation. This likely reduces visibility of internal anatomy (i.e. grey-white matter  
157 boundary), but should not significantly affect the truncation artifact, which depends primarily on the  
158 spinal cord-CSF boundary rather than internal signal variations. In conclusion, caution should be applied  
159 when interpreting hyperintensity affecting the spinal cord in T2w sagittal images of clinical patients  
160 because of the possibility that the abnormal signal could represent a truncation artifact.

## 161 **List of Author Contributions**

### 162 **Category 1**

#### 163 **(a) Conception and Design**

164 T. Gregori, R. Lam, S.L. Priestnall, C.R. Lamb

#### 165 **(b) Acquisition of Data**

166 T. Gregori, R. Lam, S.L. Priestnall, C.R. Lamb

#### 167 **(c) Analysis and Interpretation of Data**

168 T. Gregori, R. Lam, S.L. Priestnall, C.R. Lamb

- 169 **Category 2**
- 170 **(a) Drafting the Article**
- 171 T. Gregori, R. Lam, S.L. Priestnall, C.R. Lamb
- 172 **(b) Revising Article for Intellectual Content**
- 173 T. Gregori, R. Lam, S.L. Priestnall, C.R. Lamb
- 174 **Category 3**
- 175 **(a) Final Approval of the Completed Article**
- 176 T. Gregori, R. Lam, S.L. Priestnall, C.R. Lamb

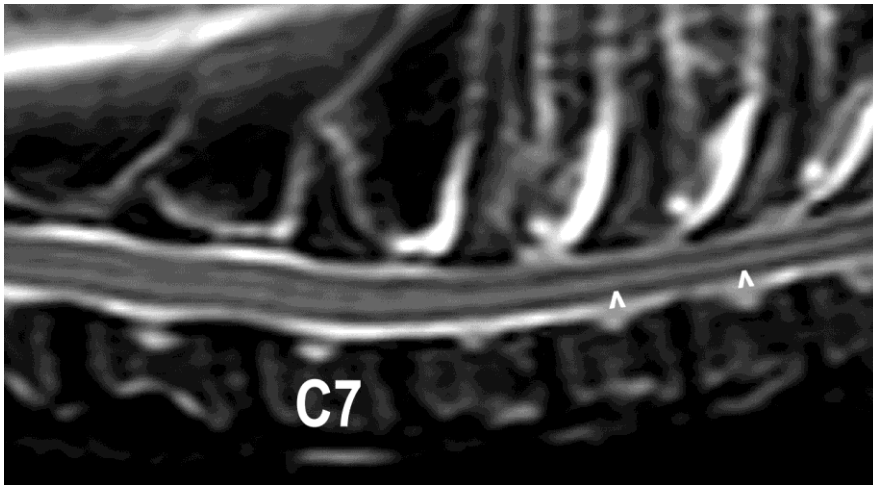
177 **References**

- 178 1. Schenck JF. Willard Gibbs and the Gibbs phenomenon. *Am J Roentgenol* 1989;152:1127-1128.
- 179 2. Lufkin RB. *The MRI Manual*. 2nd edition. St Louis: Mosby; 1998, pp121-124.
- 180 3. Bronskill MJ, McVeigh ER, Kucharczyk W, Henkelman RM. Syrinx-like artifacts on MR images of the  
181 spinal cord. *Radiology* 1988;166:485-488.
- 182 4. Frank LR, Brossmann J, Buxton RB, Resnick D. MR imaging truncation artifacts can create a false  
183 laminar appearance in cartilage. *Am J Roentgenol* 1997;168:547-554.
- 184 5. Morelli JN, Runge VM, Ai F, Attenberger U, Vu L, Schmeets SH, Kirsch JE. An image-based approach  
185 to understanding the physics of MR artifacts. *Radiographics* 2011;31:849-866.
- 186 6. Gavin PR, Bagley RS. *Practical Small Animal MRI*. Oxford: Wiley-Blackwell, 2009, p26.
- 187 7. De Decker S, Gielen IM, Duchateau L, Lang J, Dennis R, Corzo-Menendez N, Van Ham LM.  
188 Intraobserver and interobserver agreement for results of low-field magnetic resonance imaging in  
189 dogs with and without clinical signs of disk-associated wobbler syndrome. *J Am Vet Med Assoc*  
190 2011;238:74-80.
- 191 8. Allett B, Broome M.R, Hager D. MRI of a split cord malformation in a German shepherd dog. *J Am*  
192 *Anim Hosp Assoc* 2012; 48:344-351.
- 193 9. Arena L, Morehouse HT, Safir J. MR imaging artifacts that simulate disease: how to recognize and  
194 eliminate them. *Radiographics* 1995;15:1373-1394.
- 195 10. mri-q.com [Internet]. North Carolina: MRIQUESTIONS.COM, Allen D. Elster, and ELSTER LLC;  
196 [updated 2014; cited 2016 Jan 24]. Available from: <http://www.mri-q.com>
- 197 11. Block KT, Uecker M, Frahm J. Suppression of MRI truncation artifacts using total variation  
198 constrained data extrapolation. *Int J Biomed Imaging* 2008; 2008:184123.

- 199 12. Turner DA, Rapoport MI, Erwin WD, McGould M, Silvers RI. Truncation artifact: a potential pitfall in  
200 MR imaging of the menisci of the knee. *Radiology* 1991; 179:629-633.

201 **Legends**

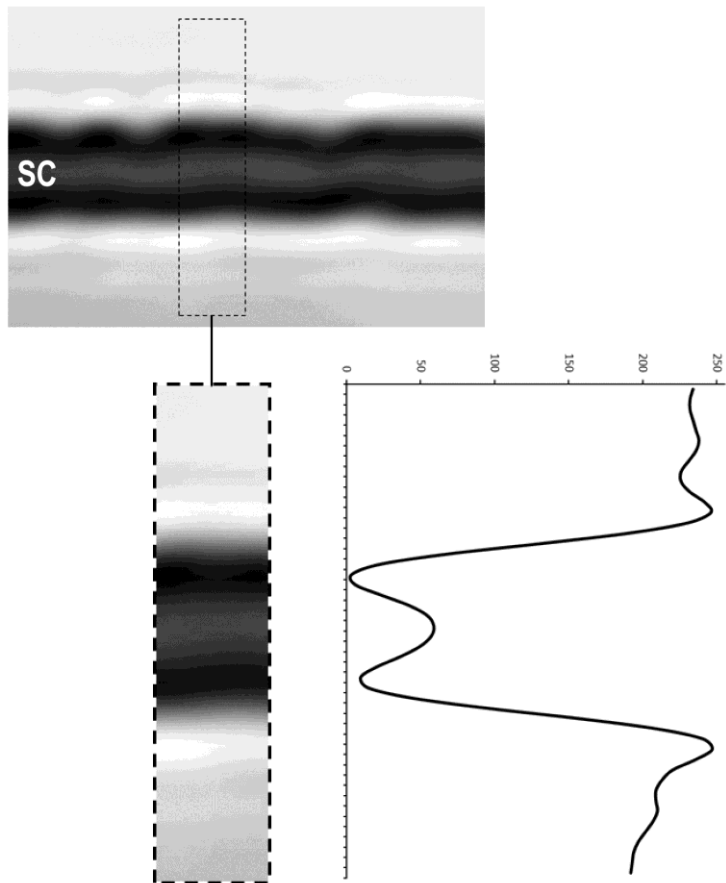
202 Figure 1. Example of a truncation artifact mimicking the central canal in a T2w sagittal image of the  
203 caudal cervical and cranial thoracic spine of a dog with surgically-confirmed thoracolumbar  
204 intervertebral disc extrusion (not shown). A centrally-located hyperintense line (arrowheads) within the  
205 thoracic spinal cord is suggestive of the central canal, but cranial to the first thoracic vertebra it splits  
206 into two lines; therefore, this line cannot represent the central canal.



207

208

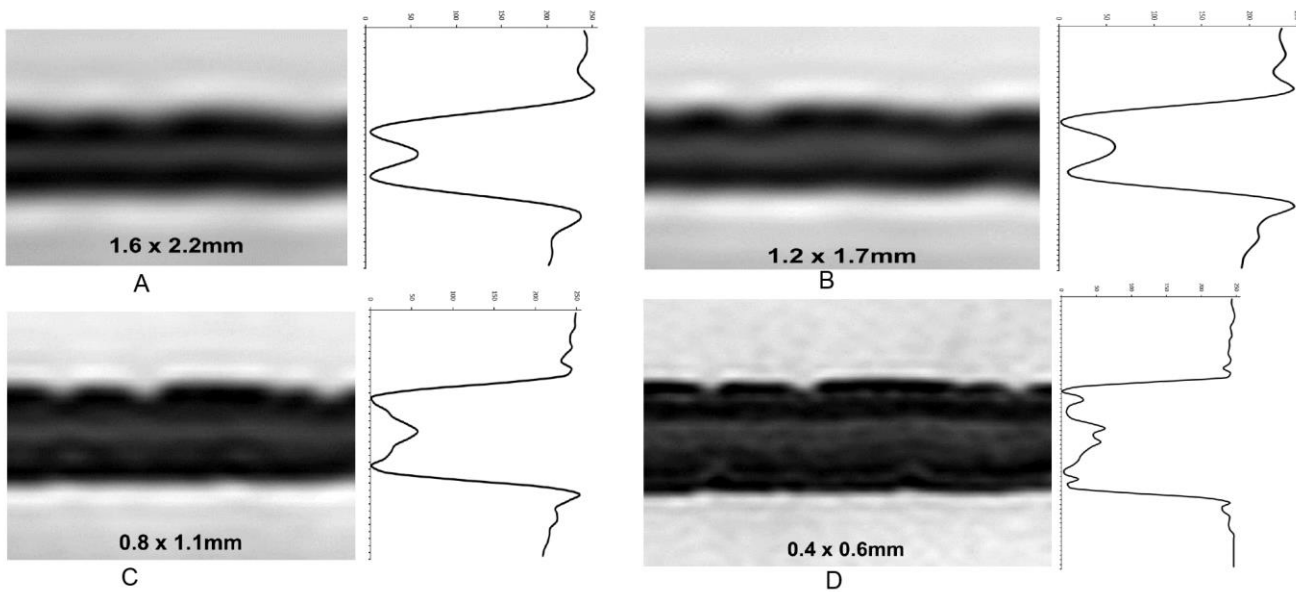
209 Figure 2. Representative T2w sagittal image of fixed spinal cord, region selected for determination of  
210 average pixel value, and corresponding graph of pixel value across the spinal cord.



211

212

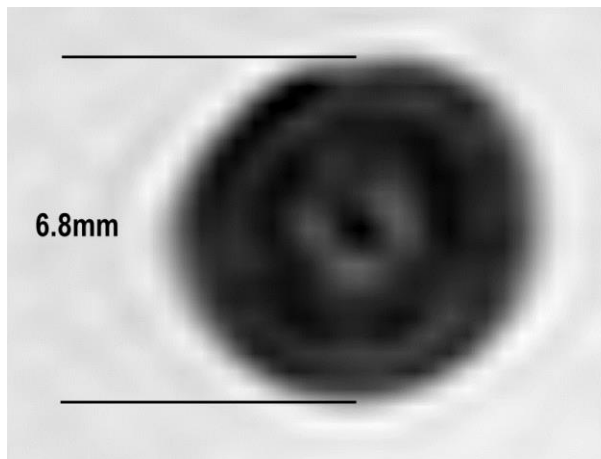
213 Figure 3. Examples of T2w MR images of fixed spinal cord obtained with the following pixel sizes: A,  
214 1.6mm (vertical) x 2.2mm (horizontal); B, 1.2mm x 1.7mm; C, 0.8mm x 1.1mm; D, 0.4mm x 0.6mm. The  
215 abnormal signal within the spinal cord that represents the truncation artifact appears as a single, wide  
216 central zone in low spatial resolution images (A & B) and as multiple narrower zones in images with  
217 higher spatial resolution (D).



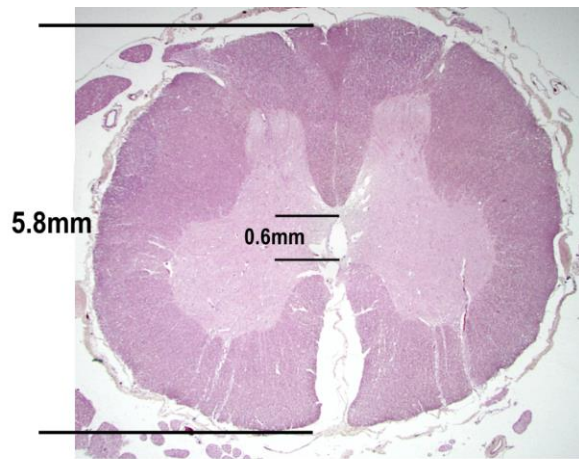
218

219

220 Figure 4. A) Transverse image of the spinal cord acquired using the same spatial resolution as series A.  
221 Multiple concentric, alternating zones of increased and decreased signal intensity are evident,  
222 representing truncation artifact associated with the curved spinal cord-fluid interface. B) Corresponding  
223 section of the cord. In the MR image, the spinal cord appears larger in diameter and the central canal is  
224 not visible.



A



B

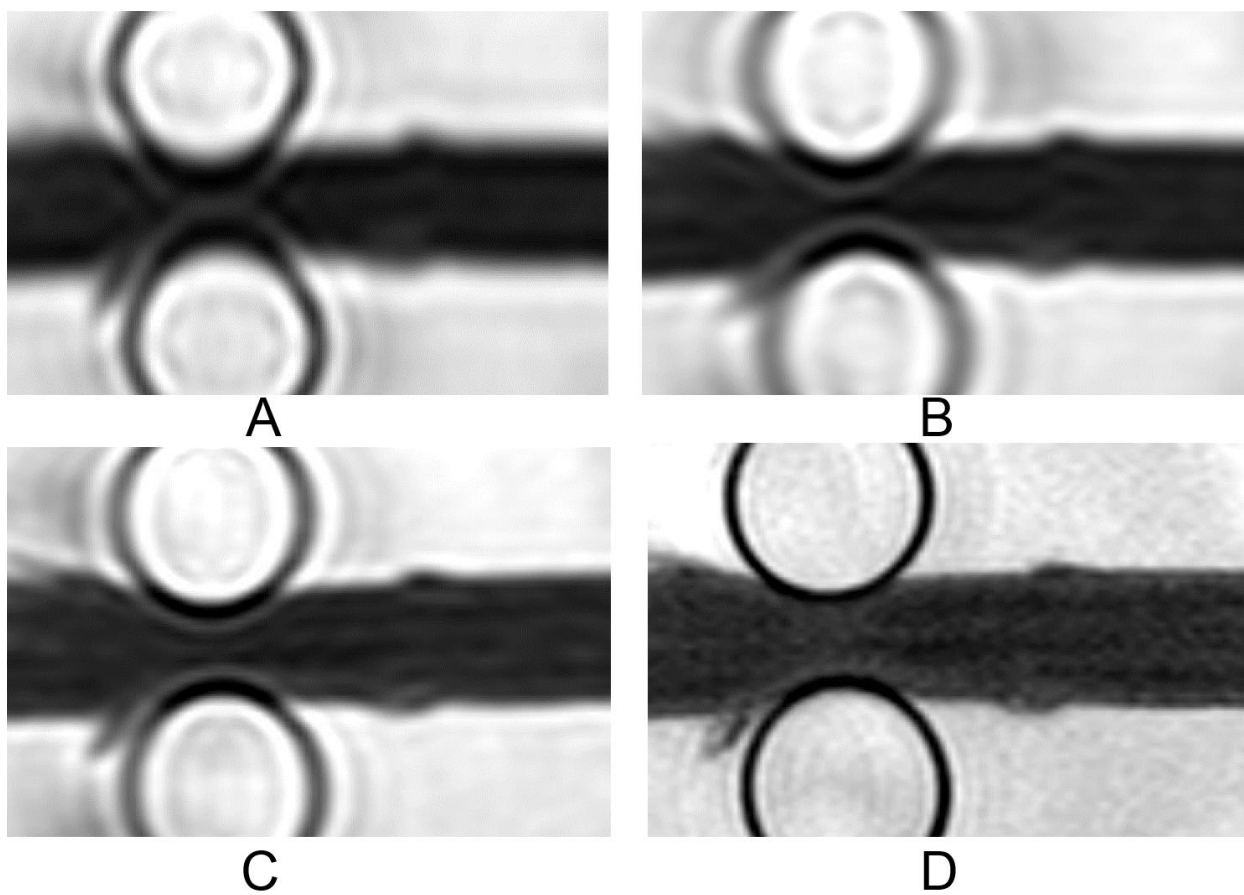
225

226

227



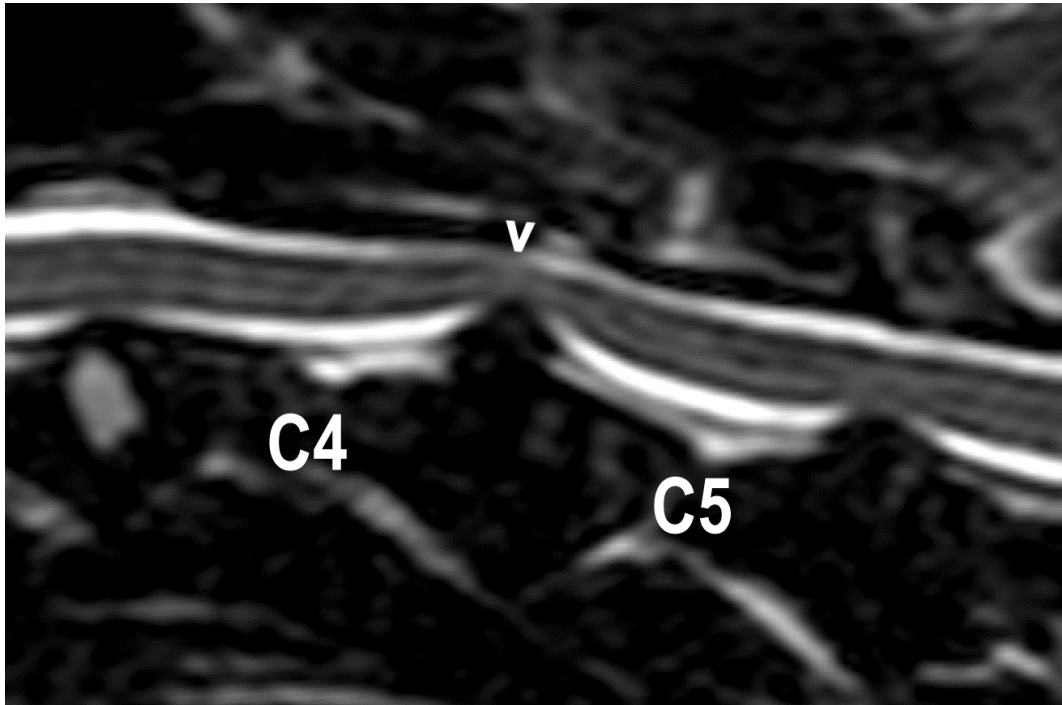
228 Figure 5. Examples of T2w MR images of unfixed, focally compressed spinal cord in a saline bath  
229 obtained with the following pixel sizes: A, 1.6mm (vertical) x 2.3mm (horizontal); B, 1.1mm x 1.5mm; C,  
230 0.8mm x 1.1mm; D, 0.4mm x 0.5mm. In the lower resolution images (A-C), concentric truncation  
231 artifacts emanating from the two syringe barrels overlap the spinal cord, impeding evaluation of its  
232 signal intensity at the site of compression. In the highest resolution image (D), the spinal cord at the site  
233 of compression had slightly increased signal intensity, apparently as a result of convergence of  
234 hyperintense truncation artifacts arising from the dorsal and ventral surfaces of the cord.



235

236

237 Figure 6. T2w sagittal image of the cervical spine of a dog with surgically-confirmed intervertebral disc  
238 extrusion at C4/5. At the site of disc extrusion (arrowhead) the cord is displaced dorsally and is narrowed  
239 compatible with compression and is relatively hyperintense. Although this hyperintensity could  
240 represent a spinal cord lesion, it is possible that it is formed by the convergence of hyperintense  
241 truncation artifacts arising from the dorsal and ventral surfaces of the cord.



242